

## 28. VRM STUDIES IN LEG 37 IGNEOUS ROCKS<sup>1</sup>

D. V. Kent, Lamont-Doherty Geological Observatory, Columbia University, Palisades, New York  
and  
W. Lowrie, Institut für Geophysik, ETH—Hönggerberg, CH-8049 Zürich, Switzerland

### ABSTRACT

A representative set of igneous rock samples from Hole 332B and Sites 334 and 335 were studied to determine their ability to acquire viscous remanence (VRM). The results for samples from Sites 334 and 335 indicate that VRM cannot be considered to be a serious secondary component in the remanence of these rocks; these samples have stable magnetizations characterized by high median destructive fields (MDF). The ability to develop VRM is quite variable in samples from Hole 332B. In high MDF samples, the developed VRM is of low intensity, but in samples with low MDF and VRM can account for a large portion of the measured NRM intensity. The quantities VRM/NRM and MDF were approximately inversely proportional for samples from the three holes studied here.

### INTRODUCTION

Some magnetic properties, including the acquisition of viscous remanent magnetization (VRM), were studied in a limited number (16) of Leg 37 igneous rock samples. Ten samples were available from Hole 332B, two samples from Site 334, and four samples from Site 335. Most samples are of basaltic rock although at least one sample (from Site 334) is of ultramafic composition.

### REMANENT MAGNETIC PROPERTIES

The NRM intensity and direction of each sample were measured with a Digico complete results spinner magnetometer, and the weak-field susceptibilities were measured with an a.c. bridge (Figure 1). The geometric mean NRM intensity is  $2.7 \times 10^{-3}$  Gauss and the mean susceptibility is  $6.9 \times 10^{-4}$  G/oe, similar to the mean values of  $2.1 \times 10^{-3}$  Gauss and  $6.3 \times 10^{-4}$  G/oe, respectively, reported for 26 DSDP sites by Lowrie (1974). The  $Q'_n$  ratios are (with one exception at Site 334) greater than unity (Chapters 2, 4, and 5, this volume).

The remanence of each sample was progressively demagnetized in alternating fields to at least 400 oe. In general, the remanent directions were very stable during AF demagnetization (Figure 2), although in some samples the data quality deteriorated in fields greater than 800 oe, due probably to the acquisition of anhysteretic remanence (ARM) components. From each demagnetization curve the median destructive field (MDF) was determined, as well as the stable direction. In the site report chapters the declinations and inclinations of NRM and the stable direction are compared, although the declinations themselves have no

absolute meaning because of the absence of azimuth orientation.

The NRM intensities and inclinations are very similar to those measured in nearby samples onboard ship (Table 1 and Ade-Hall, 1974; personal communication). Both sets of paleomagnetic data indicate the occurrence of both normal and reversed polarity zones within basement rocks penetrated by Hole 332B and Site 334; the four samples from Site 335 have uniform negative inclinations, slightly steeper than the expected axial dipole field inclination for the site latitude.

### THERMOMAGNETIC ANALYSIS

Thin slices from each sample were ground to a fine powder for Curie temperature studies. These experiments were carried out in air with a vertical motion Curie balance, the field (4 koe) being switched off frequently to monitor possible weight loss in the specimens. The thermomagnetic curves were mostly irreversible (Figure 3a) and have the general character typical of oceanic basalts in which titanomagnetites are frozen in a metastable condition by rapid chilling (Ozima and Ozima, 1971). The Curie temperature ( $\theta_i$ ) of the initial mineral (titanomagnetite) is lower than that of the exsolved magnetite ( $\theta_f$ ), and the initial room temperature magnetization ( $J_i$ ) is less than the final room temperatures magnetization ( $J_f$ ), so that ( $J_i/J_f$ ) is typically less than unity (Table 2).

In two samples (332B-45-1, 104 cm and 334-26-1, 140 cm) the curves were almost reversible, apart from some high temperature oxidation, and show none of the irreversibility associated with titanomagnetite phase separation. The Curie temperatures of these samples are similar to the values of  $\theta_f$  for the other samples, corresponding to a magnetite containing a slight amount of titanium. Sample 332B-45-1, 104 cm is from a com-

<sup>1</sup>Institut für Geophysik Contribution No. 118.

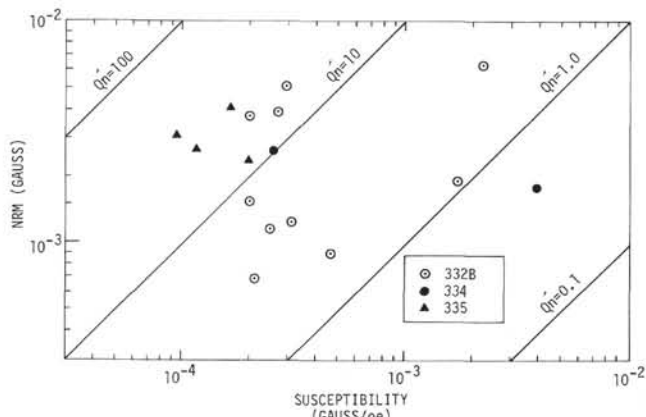


Figure 1. NRM intensities and susceptibilities of the basalt samples.

plex brecciated unit of basalt near the base of Hole 332B whereas Sample 334-26-1, 140 cm is from an ultramafic unit (near the base of Site 334) containing in part serpentinized peridotite. We infer that the occurrence of magnetite in these samples was due to either exsolution of titanomagnetite carried to completion in situ or to secondary formation of magnetite, particularly in the serpentinized peridotite (Saad, 1969). The latter explanation can help to account for the mixed remanent polarities encountered at Site 334 if the secondary magnetite formed and acquired a chemical remanent magnetization in a magnetic field different from that recorded by the overlying basaltic rocks.

In 10 of the 16 thermomagnetic curves, an initial increase in magnetization was observed (e.g., Figure 3a,

Table 2), as also reported by Ade-Hall (1974) in some Leg 26 basalts and attributed to a possible low temperature chemical change. In two specimens incomplete exsolution was observed; in 332B-9-2, 92 cm a

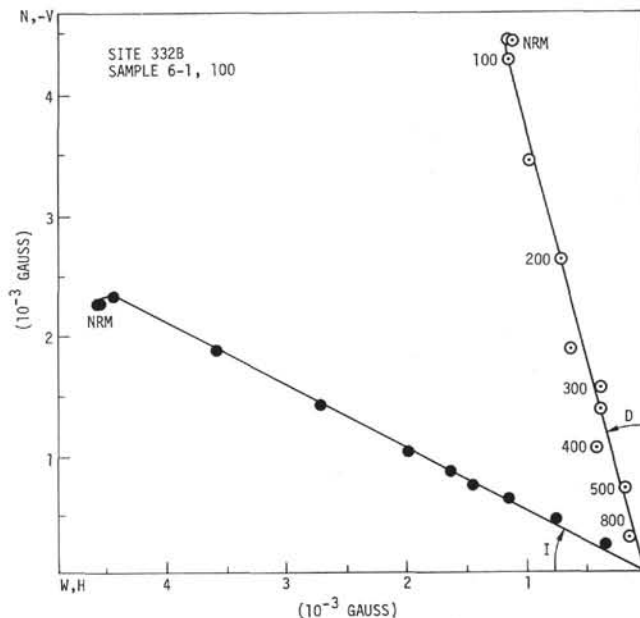


Figure 2. Vector diagram showing stability against AF demagnetization of the declination (D), defined by N and W (open dots), and the inclination (I), defined by V and H (solid dots) in DSDP Leg 37 oceanic basalt. The numbers indicate the AF intensity in peak oersted.

TABLE 1  
Comparison of NRM Intensities and Inclinations Measured in the Laboratory With Shipboard Measurements in Nearby Samples

Laboratory			Shipboard			
Sample (Interval in cm)	Intensity (10 <sup>-4</sup> Gauss)	Inclination	Approx. Subbasement Depth (m)	Sample (Interval in cm)	Intensity (10 <sup>-4</sup> Gauss)	Inclination
<b>Hole 332B</b>				<b>Hole 332B</b>		
2-5, 113	9.05	-11	18	2-5, 106	7.62	13
6-1, 100	50.9	-26	144	6-1, 77	43.9	-38
9-2, 92	12.5	20	192	9-2, 104	23.3	39
11-1, 110	19.2	40	220	11-1, 39	19.8	26
14-2, 84	7.02	48	249	14-2, 81	13.1	42
17-1, 6	36.8	-31	276	18-1, 43	53.0	-29
22-4, 48	38.6	-8	328	22-4, 40	38.6	-5
27-2, 112	15.3	18	373	27-2, 4	35.0	-11
33-1, 127	11.4	-43	429	33-1, 100	8.2	-30
45-1, 104	63.4	-4	543	45-1, 104	74.3	-2
<b>Site 334</b>				<b>Site 334</b>		
9-2, 70	26.2	65	40	17-1, 17	18.5	41
26-1, 140	17.8	-23	106	26-1, 20	21.4	-77
<b>Site 335</b>				<b>Site 335</b>		
6-5, 33	41.3	-63	10	6-3, 108	64.1	-69
9-4, 58	24.3	-61	37	9-5, 94	27.4	-71
10-3, 76	31.1	-65	45	10-3, 76	43.2	-60
13-2, 13	27.1	-70	72	13-2, 13	15.1	-81

**TABLE 2**  
**Curie Temperature Analysis**

Sample (Interval in cm)	$\theta_i^a$	$\theta_f^b$	$J_i/J_f^c$
<b>Hole 332B</b>			
2-5, 113	255	530	0.697
6-1, 100*	245	565	0.513
9-2, 92	212	505	0.439
11-1, 110	160	—	—
14-2, 84*	290	550	0.226
17-1, 6*	300	555	0.584
22-4, 48*	270	555	0.497
27-2, 112*	240	555	0.420
33-1, 127*	280	545	0.308
45-1, 104	545	545	1.235
<b>Site 334</b>			
9-2, 70*	300	540	0.358
26-1, 140	570	555	1.590
<b>Site 335</b>			
6-5, 33*	280	550	0.330
9-4, 58*	320	550	0.428
10-3, 76*	310	545	0.388
13-2, 13	345	535	0.425

Note: Asterisks identify samples with thermomagnetic curves showing initial increase in magnetization.

<sup>a</sup>Curie temperature before heating.

<sup>b</sup>Curie temperature of final mineral.

<sup>c</sup>Ratio of initial to final magnetizations.

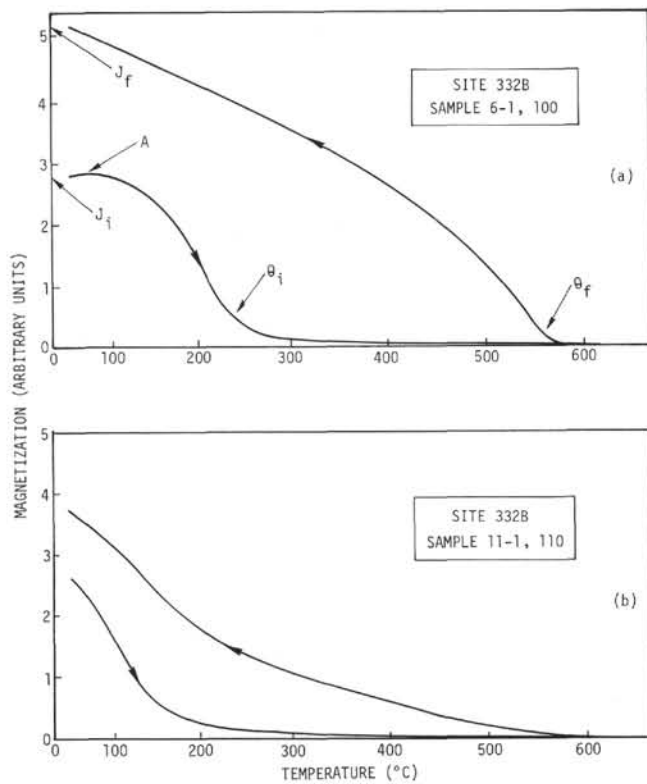


Figure 3. (a) Typical irreversible thermomagnetic curve measured in air in 4000 oe, showing the slight initial rise in magnetization (A), the initial and final magnetizations ( $J_i$  and  $J_f$ , respectively), and the initial ( $\theta_i$ ) and final ( $\theta_f$ ) Curie temperatures. (b) Thermomagnetic curve of sample in which exsolution after thermal cycling was incomplete.

Curie temperature in the cooling curve was visible near the Curie temperature of the initial mineral which was also comparatively low (210°C). In Sample 332B-11-1, 110 cm, the exsolution was so incomplete that a magnetite Curie point could not reasonably be determined (Figure 3b). The initial Curie point (160°C) is lower than any of the others, which range from 212°C to 570°C (Table 2).

Thermomagnetic curves in vacuum permit a description of the state of oxidation of titanomagnetites (Ozima and Ozima, 1971). It is possible to use thermomagnetic curves in air for this same purpose although this method is not unambiguous (Lowrie et al., 1973). Assuming at first stoichiometric titanomagnetites, the composition of the initial and final minerals may be determined from their Curie points,  $\theta_i$  and  $\theta_f$ . Appropriate initial and final magnetizations may be calculated and the expected ratio ( $J_i/J_f$ ) determined. The stoichiometric titanomagnetites should lie on the line ST in Figure 4. Points lying above this line may or may not be stoichiometric, but points lying below the line are nonstoichiometric. Thus, most of the points from Hole 332B lie above the stoichiometric line, and may be stoichiometric although this is not an unambiguous conclusion. However, the samples from Sites

334 and 335 as well as two of the Hole 332B samples, lie below the line. The only way this can occur is as a result of maghematization of the original mineralogy.

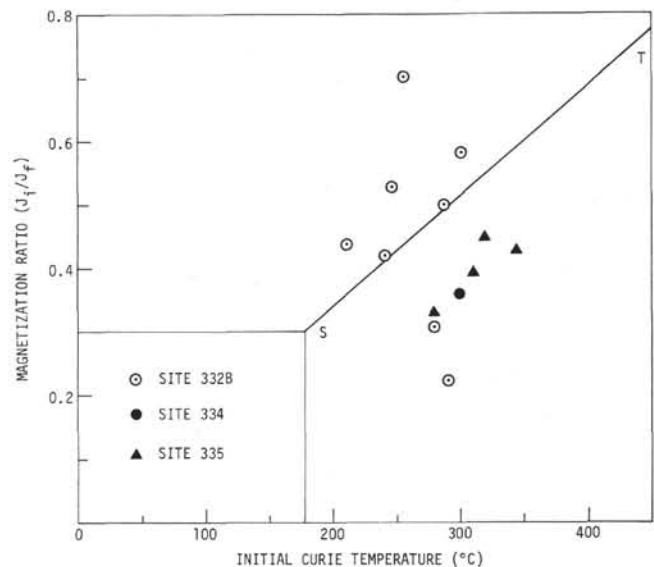


Figure 4. Plot of magnetization ratio ( $J_i/J_f$ ) against  $\theta_i$  for 13 samples. Line ST represents the stoichiometric curve; points below ST indicate the initial titanomagnetite is non-stoichiometric.

### VISCOUS REMANENT MAGNETIZATION EXPERIMENTS

The specimen magnetizations were measured after demagnetization and the specimens were placed in a uniform field of 1 oe. After 1 hr, and again at logarithmically spaced intervals for a total of about 580 hr, the remanences were remeasured, and the VRM component computed. In this way the growth of VRM in each sample was monitored. A representative VRM growth curve is shown in Figure 5, in which the acquisition appears to proceed in three distinct segments. This interpretation is consistent with observations of VRM acquisition in many other DSDP basalts (Lowrie, 1974). The growth of VRM proceeds logarithmically with time, but at different rates in each segment. Instead of attempting to determine a representative average viscosity coefficient for each curve, the VRM intensity acquired in the 1-oe field over 500 hr was used to calculate the ratio VRM/NRM for each sample; the NRM intensities, VRM intensities, and the ratio VRM/NRM are listed in Table 3. The ratio

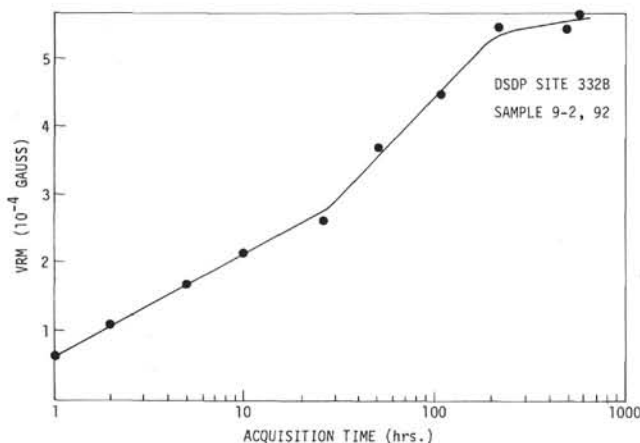


Figure 5. Acquisition of VRM in three distinct stages in a sample from Hole 332B.

VRM/NRM is an expression of the potential seriousness of the effect of VRM on the sample. It varies from about 1.5% in Sample 335-13-2, 13 cm to 79% in Sample 332B-11-1, 110 cm, and averages (geometric mean) only 8.5%. It is quite variable from sample to sample in Hole 332B without any consistent correlation with depth and is uniformly low at Site 335 where the median destructive fields are relatively high.

The VRM/NRM ratio is inversely related to the median destructive field (MDF) as shown in Figure 6. Only Samples 332B-45-1, 104 cm and 334-26-1, 140 cm appear to differ from the trend defined by the other specimens. The thermomagnetic analysis showed that these two samples have different magnetic mineralogies than the others, probably dominated by magnetite rather than titanomagnetite or titanomaghemite. In Sample 332B-45-1, 104 cm the NRM intensity and susceptibility are much higher than in the other samples, and although the actual VRM is fairly strong, it is small in proportion to the NRM. Sample 334-26-1, 140 cm is unusually coarse grained and has a

TABLE 3  
Comparison of VRM, Acquired in a Field of 1 oe for 500 hr, With NRM Intensity in Each Sample

Sample (Interval in cm)	Intensity ( $10^{-4}$ G)		
	NRM	VRM	VRM/NRM (%)
<b>Hole 332B</b>			
2-5, 113	9.05	4.35	48.0
6-1, 100	50.9	3.19	6.3
9-2, 92	12.5	4.64	37.0
11-1, 110	19.2	15.1	79.0
14-2, 84	7.02	0.49	7.0
17-1, 6	36.8	1.45	3.9
22-4, 45	38.6	2.64	6.8
27-2, 112	15.3	1.57	10.0
33-1, 127	11.4	1.42	12.0
45-1, 104	63.4	3.86	6.1
<b>Site 334</b>			
19-2, 70	26.2	1.48	5.6
26-1, 140	17.8	2.12	12.0
<b>Site 335</b>			
6-5, 33	41.3	1.04	2.5
9-4, 58	24.3	1.33	5.5
10-3, 76	31.1	1.28	4.1
13-2, 13	27.1	0.41	1.5

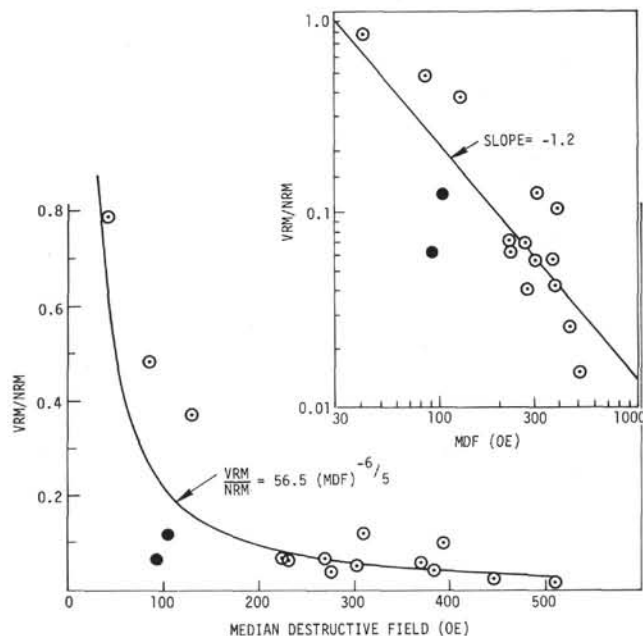


Figure 6. The ratio of the VRM acquired over 500 hr in 1 oe to the NRM intensity (VRM/NRM) plotted against median destructive field (MDF). Inset: the slope of the double logarithmic plot suggests that the best-fit relationship is approximately  $(VRM/NRM) = 56.5 (MDF)^{-6/5}$ . Solid circles are for Samples 332B-45-1, 104 cm and 334-26-1, 140 cm (see text).

high susceptibility and correspondingly low  $Q'n$  value. In this sample the VRM developed is of moderate intensity, but low in proportion to the susceptibility of the sample.

## CONCLUSIONS

It has been observed (Lowrie and Kent, 1975) that VRM acquired from the NRM state can be developed almost twice as rapidly as from the demagnetized state. Nevertheless, the present results indicate such low amounts of VRM from the demagnetized state in samples from Sites 334 and 335 that VRM cannot be considered to be a serious component in the remanence of the basaltic layer at these sites. These sites have stable magnetizations characterized by high median destructive fields.

In Hole 332B, however, the ability to develop VRM is quite variable. In high MDF samples the developed VRM is generally of low intensity, but in samples with low MDF the VRM (especially in the NRM state) ought to be able to account for a large portion of the measured NRM intensity. The inverse relationship between NRM/VRM and MDF follows an approximately  $-6/5$  power law (Figure 6), or, to a rougher approximation, the two quantities are inversely proportional.

No attempt has been made to analyze the shapes of the VRM acquisition curves, which for experimental reasons were in many cases not of sufficiently high quality to permit separation of each curve into more than one distinct stage as shown in Figure 5. The sample illustrated indicates, however, that, as reported in many other DSDP basalts (Lowrie, 1974), VRM is not usually carried in these rocks by a single phase. It is apparent from thermomagnetic analysis that many samples may be at least partially oxidized, and that both titanomagnetite and titanomaghemite may be present. This would allow VRM to be acquired by two distinct minerals in such samples at the two different observed rates.

Where only a single mineralogical phase is present (titanomagnetite or titanomaghemite), it would be possible for two grain-size fractions to contribute differently to the VRM. For example, the center of the three acquisition stages in Figure 4 evidently corresponds to a discrete range of activation times which,

after initiation, are fairly quickly exhausted. It is not possible on the basis of present data to satisfactorily explain these phases, or to say whether other discrete ranges exist beyond the limits of the period of experimental observation. If this is not the case, and the rate of VRM acquisition observed in the latest stage is taken to be representative for longer periods of time, then it appears that a large portion of VRM is acquired by the time the second stage has passed, in comparison to the VRM that might be acquired during very long times, of the order of the duration of a geomagnetic polarity epoch.

## ACKNOWLEDGMENTS

We are grateful to N.D. Opdyke and R.L. Larson for critically reading the manuscript and to M.N. Israfil and M. Sundvik for technical assistance in the laboratory. The work was supported by National Science Foundation Grant DES 74-17965.

## REFERENCES

- Ade-Hall, J.M., 1974. Strong field magnetic properties of basalts from DSDP Leg 26. *In* Davies, T.A., Luyendyk, B.P., et al., Initial Reports of the Deep Sea Drilling Project, Volume 26: Washington (U.S. Government Printing Office), p. 529-532.
- Lowrie, W., 1974. Oceanic basalt magnetic properties and the Vine and Matthews hypothesis: *Zeit. für Geophysik/J. Geophys.*, v. 40, p. 513-536.
- Lowrie, W. and Kent, D.V., 1975. Viscous remanent magnetization in basalt samples. *In* Hart, S.R., Yeats, R.S., et al., Initial Reports of the Deep Sea Drilling Project, Volume 34: Washington (U.S. Government Printing Office), p. 479-484.
- Lowrie, W., Løvlie, R., and Opdyke, N.D., 1973. Magnetic properties of Deep Sea Drilling Project basalts from the North Pacific Ocean: *J. Geophys. Res.*, v. 78, p. 7647-7660.
- Ozima, M. and Ozima, M., 1971. Characteristic thermomagnetic curve in submarine basalts: *J. Geophys. Res.*, v. 76, p. 2051-2056.
- Saad, A.H., 1969. Magnetic properties of ultramafic rocks from Red Mountain, California: *Geophysics*, v. 34, p. 974-987.